World Academy of Science, Engineering and Technology
International Journal of Industrial and Manufacturing Engineering
Vol:6, No:11, 2012

Experimental Study on Machinability of Laser-Sintered Material in Ball End Milling

Abdullah Yassin, Takashi Ueda, and Syed Tarmizi Syed Shazali

Open Science Index, Industrial and Manufacturing Engineering Vol:6, No:11, 2012 publications.waset.org/12176/pdf

***Abstract*—**This paper presents an experimental investigation on the machinability of laser-sintered material using small ball end mill focusing on wear mechanisms. Laser-sintered material was produced by irradiating a laser beam on a layer of loose fine SCM-Ni-Cu powder. Bulk carbon steel JIS S55C was selected as a reference steel. The effects of powder consolidation mechanisms and unsintered powder on the tool life and wear mechanisms were carried out. Results indicated that tool life in cutting laser-sintered material is lower than that in cutting JIS S55C. Adhesion of the work material and chipping were the main wear mechanisms of the ball end mill in cutting laser-sintered material. Cutting with the unsintered powder surrounding the tool and laser-sintered material had caused major fracture on the cutting edge.

***Keywords*—**Laser-sintered material, tool life, wear mechanism.

I. Introduction

A MILLING-combined laser sintering system (MLSS), which is a rapid tooling machine that combines laser assisted metal sintering and high speed end mill has made a complicated injection mould that allows the creation of a deep rib. With MLSS, the dimensional accuracy is improved and a cooling channel can be easily created. For instance, machining of spiral holes along the mold profile, which is difficult in the conventional machining process can be made using MLSS [1]. Therefore, it is important to study the tool wear mechanisms of sintered materials, if we want to take advantage of MLSS as a new invention in making complicated injection molds in a shorter time. Yassin et al. [2] investigated the machinability of a sintered material focussing on specific cutting energy and tool flank temperature. The results showed that the machinability of the sintered material is lower compared with JIS S55C. In this paper, tool life and tool wear mechanisms were investigated. It is crucial to investigate tool life when cutting sintered materials because tool wear could greatly influence the dimensional accuracy and surface finish. Besides that, the flank wear and the corresponding cutting edge temperature were measured.

Abdullah Yassin is with the Department of Mechanical Engineering and Manufacturing, Faculty of Engineering, Universiti Malaysia Sarawak, Kota Samarahan 94300 Sarawak, Malaysia (Phone: +6082583340, fax +6082583410; email: yabdulla@feng.unimas.my)

Takashi Ueda is with the Institute of Science and Engineering, Kanazawa University,Kakuma-machi, Kanazawa, Ishikawa 920-1192, Japan (Phone : +81-76-234-4724, fax : +81-76-234-4725; email: ueda@se.kanazawa-u.ac.jp)

Syed Tarmizi Syed Shazali is with the Department of Mechanical Engineering and Manufacturing, Faculty of Engineering, Universiti Malaysia Sarawak, Kota Samarahan 94300 Sarawak, Malaysia (Ph one: +608258271, fax +6082583410; email: starmizi@feng.unimas.my).

II. Milling-Combined Laser Sintering System (MLSS)

In MLSS, the apparatus for laser sintering consists of a continuous wave Yb:Fiber laser ($\lambda = 1.07$ μm) with a maximum output power of 200 W, laser spot diameter of 94 μm and maximum laser scanning speed of 1000 mm/sec. The apparatus for high speed milling consists of a spindle with maximum rotational speed of 50000 rpm and maximum feed speed 1000 mm/min.

Two alternating processes occur in MLSS, namely, forming a layer profile by laser sintering and surface finishing by high speed milling. Fig. 1 illustrates the concept of the MLSS. The process of MLSS can be summarized as follows. A 3-D model is designed using CAD and is divided into sliced layers whose thickness is 50 μm. Then, this model is transferred to the MLSS. Prior to the laser sintering process, a sandblasted steel base plate is placed on the building platform. Next, a predetermined layer thickness of 50 μm of loose metallic powder is spread on the base plate using a recoating blade. Successively, the laser beam is irradiated to the surface of a layer of loose metallic powder and this will produce a layer-wise profile according to the CAD data of the sliced layer, see Fig. 1(a). After forming a few layers of sintered material, the milling process is executed at the periphery surface as shown in Fig. 1(b). The sintering and milling at the periphery surface are repeated whereas the top surface is not cut after all layers are sintered. The laser sintering and cutting processes are performed in a nitrogen atmosphere at room temperature to prevent oxidization.

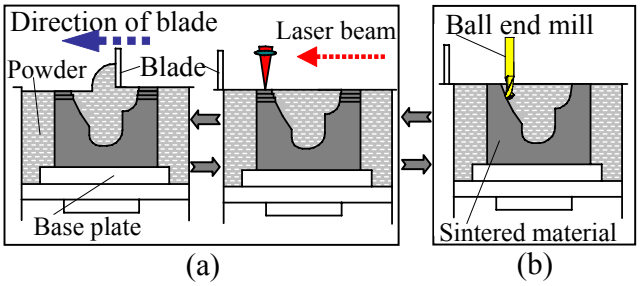


Fig. 1 Concept of milling-combined laser sintering system (MLSS) (a) forming layers and (b) high speed milling

Open Science Index, Industrial and Manufacturing Engineering Vol:6, No:11, 2012 publications.waset.org/12176/pdf

III. Sintered Material

TABLE I
PROPERTIES OF METALLIC POWDER

Material		SCM	Ni	Cu
Particle diameter	μm	30	30	30
Powder density	kg/m^3	4690	4040	4690
Specific heat	J/g.K	0.45	0.49	0.38
Thermal conductivity	W/m.K	0.13	0.17	0.17

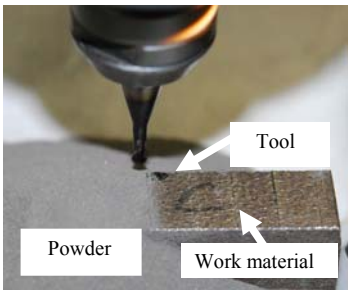


Fig. 2 Experimental set-up in cutting laser-sintered material with unsintered powder

Table I gives the properties of the metallic powder used to produce a sintered part. The metallic powder mixture consists of 70 wt.% SCM, 20 wt.% Ni and 10 wt.% Cu. The work material was made by the MLSS without executing the milling process and is denoted as $E_{\rho 9}$ in this paper.

In order to investigate the influence of powder consolidation mechanisms and unsintered powder, three conditions are defined; that is inner surface, $E_{\rho 9}$ (y=1), outer surface, $E_{\rho 9}$ (y=0), and unsintered powder surrounding outer surface, $E_{\rho 9}$ (y=0+powder), see Fig. 2. The outer surface is a surface in which the unmolten and partially molten powder remained on the surface while the inner surface is a surface in which the metallic powder melted completely. The hardness and density of the $E_{\rho 9}$ material are 275 HV(0.3), and 7680 kg/m^3, respectively [2].

IV. Experimental Procedures

TABLE II
EXPERIMENTAL CONDITIONS FOR TOOL WEAR MEASUREMENT

Tool material	Coated cemented carbide
Diameter	2.0 mm
Spindle rotation	N: 30000 rpm
[Cutting speed]	V :188 m/min
Feed per tooth	f : 0.01 mm/tooth
Feed speed	f_s : 600 mm/min
Axial depth of cut	Ad: 0.1 mm
Radial depth of cut	Rd: 0.4 mm
Cutting method (Down cut without cutting fluid)	Peripheral milling

The experiments were carried out using an air spindle unit machine. Table II gives the cutting parameters for tool wear measurement. Maximum flank wear width was measured using a micrometer-equipped microscope. This was plotted against cutting time and cutting was stopped when the flank wear reached a value of 200 μm. Worn out tools were further examined using a scanning electron microscope (SEM).

Cutting edge temperature was measured by using a three-color pyrometer with an optical fiber, and it has a flat response to about 500 kHz. This pyrometer has enough response speed to measure cutting edge temperature of the tool, which is rotating at high revolution speed [3]. Same experimental set-up as reported in [4] was used in this research to measure cutting edge temperature.

V. Experimental Results and Discussion

A. Tool Wear Mechanisms

Fig. 3 shows the progress of the maximum height of wear on the flank face Vb_{max} in cutting $E\rho_9$ (y=0+powder), $E\rho_9$ (y=0), $E\rho_9$ (y=1), and JIS S55C. At the initial cutting stage, Vb_{max} in cutting all work materials were almost same. In cutting $E\rho_9$ (y=0+powder), major fracture was observed at the cutting edge after it underwent approximately 7 min cutting time, hence the Vb_{max} increased drastically, see Fig. 3. The formation of fracture occurred because of the existence of unsintered metallic powder. Cutting with the fine unsintered powder surrounding the work material increased the specific cutting energy and cutting temperature. This indicates a possibility that the fine unsintered metallic powders appear between the flank face and the machined surface. When this occurs, the cutting edge experiences a high stress and cutting temperature, consequently a severe fracture occurs. With regard to cutting $E\rho_9$ (y=0) and $E\rho_9$ (y=1), adhesion of the $E\rho_9$ work material was found on the flank face, demonstrating a strong bond at the work material-tool interface. The formations of the adhered $E\rho_9$ material onto the flank face were probably due to the high temperature at the cutting zone. A similar conclusion is reported in [5]. Due to the dynamics of the milling process, the cutting edge experienced thermal shock at every rotation and the layers of adhered work material was cyclically removed and replaced. The strong bonding strength between tool materials and the adhered layers cause the hard particles of the tool material to be carried away from the tool, hence an abrasive action and micro chipping occur. With prolonged cutting, the layer of adhered work material become larger, see Fig. 3. When this large adhered layer becomes unstable, it will be removed from the tool and cause a big volume of hard particles of the tool material to be carried away from the tool, hence macro chipping occurs and Vb_{max} increases drastically. As reported earlier in [4], cutting at the outer surface of the laser-sintered material generates higher specific cutting energy and temperature due to the existence of partially molten powder on the outer surface. Increasing specific cutting energy will result in higher stress, therefore, the greater cutting edge temperature and stress generated on the flank face probably reduces the

yield strength of the tool, leading to a higher rate in wear and micro chipping. Therefore, the cutting tool reached its end tool life early in cutting Eρ9 (y=0) then followed by

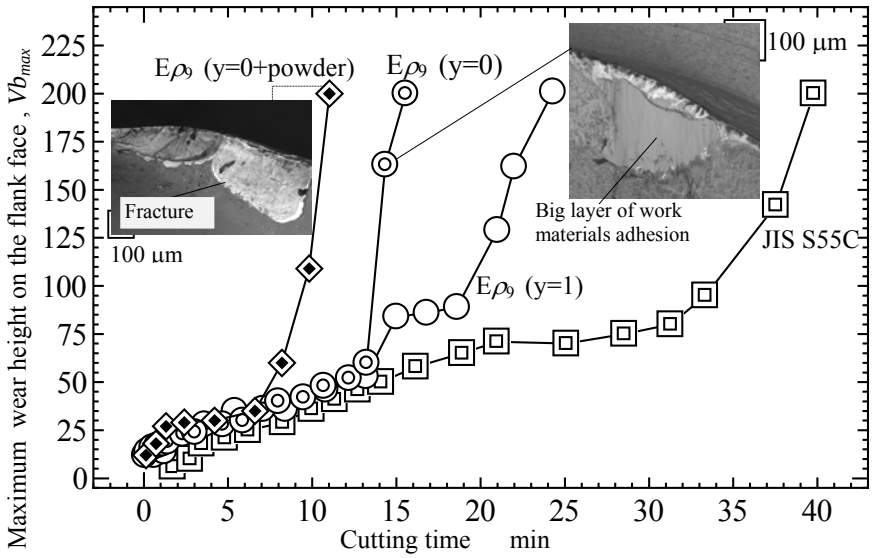


Fig. 3 Progress of the maximum wear height on the flank face, Vb_{max}

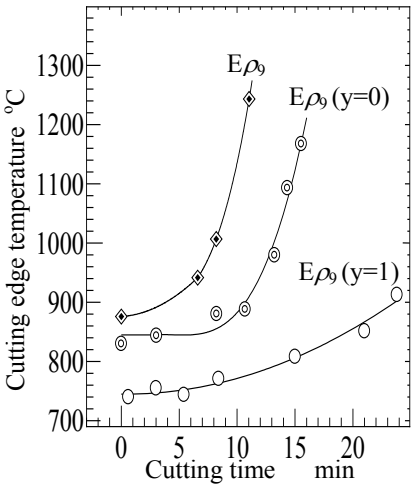


Fig. 4 The evolution of the cutting edge temperature with cutting time

(y=1).With respect to cutting JIS S55C, mechanical wear was observed at the initial cutting stage. As cutting progressed, mechanical wear tended to be suppressed and thermal wear took place.

B. Cutting Edge Temperature Evolution

During the cutting process, the wear on the flank face and the corresponding cutting edge temperature were measured. Fig. 4 shows the evolution of the maximum cutting edge temperature during the tool life in cutting Eρ9 (y=0+powder), Eρ9 (y=0), and Eρ9 (y=1). Cutting edge temperature in cutting Eρ9 (y=0+powder) increased drastically when the cutting time reached 8 min and show a similar trend to the corresponding wear curve as shown in Fig. 3. The highest cutting edge temperature of 1240 °C was obtained in cutting Eρ9 (y=0+powder) at the cutting time 11 min. This is probably due to the fracture at the tip of the cutting edge. With regard to Eρ9 (y=0), the maximum cutting edge temperature of 1170 °C was recorded at the cutting time 16 min. The same observation was obtained in the wear curve. This is because when the cutting edge cut the partially molten powder, the cutting edge that had a chipping generated a high temperature. With regard to Eρ9 (y=1), the maximum cutting edge temperature of 910 °C was recorded at the cutting time 24 min. The difference of recorded maximum temperature between Eρ9 (y=0) and Eρ9 (y=1) was approximately 260 °C. This big difference is probably due to the effect of powder consolidation mechanisms. For Eρ9 (y=1), almost all metallic powder experience a full melting and for Eρ9 (y=0), some metallic powders are not fully melted. Partially molten powder is superior to fully molten powder in showing greater hardness. The cutting edge temperature evolution can provide valuable information on thermal effects in relation to the final work material characteristics.

VI. Conclusion

The investigation of tool wear mechanism was carried out experimentally. The effect of unsintered powder on tool life was examined. Besides that, cutting edge temperature corresponding to tool wear is discussed. It has shown that tool life in cutting laser-sintered material is lower than that in cutting JIS S55C. The tool life in cutting Eρ9 material and JIS S55C can be arranged in this ascending order: Eρ9 (y=0+powder), Eρ9 (y=0), Eρ9 (y=1), and JIS S55C. Non-uniform wear is the dominant wear pattern of the ball end mill in cutting laser-sintered material. As for JIS S55C, uniform flank wear was observed at the initial stage and this uniform flank wear tends to disappear as cutting progresses. In cutting Eρ9 (y=0+powder), cutting tool experienced fracture at early cutting time. The formation of the adhered work material onto the flank face in cutting Eρ9 material caused a micro chipping on the tool. When the adhered layer became bigger and unstable, macro chipping occurs. The wear of cutting tool has a substantial effect on the cutting edge temperature. It has shown that as wear evolved with cutting time, the corresponding cutting edge temperature shows a continuous increase because of larger contact surfaces between the work material and the cutting tool.

Acknowledgment

This research was partially funded by Universiti Malaysia Sarawak via Small Grant Scheme (02(S87)/826/2011(21)).

Open Science Index, Industrial and Manufacturing Engineering Vol:6, No:11, 2012 publications.waset.org/12176/pdf

REFERENCES

[1] Abe, S., *Study on Development of Milling-Combined Laser Metal Sintering System and Production of Injection Molds*, in *Department of Mechanical System Engineering*. 2008, Kanazawa University: Kanazawa, Ishikawa, Japan. p. 180.

[2] Yassin, A., et al., *Study on Cutting Characteristics of Sintered Material with Yb: Fiber Laser.* Journal of Advanced Mechanical Design, Systems, and Manufacturing, 2008. **2**(5): p. 833-843.

[3] Ueda, T., A. Hosokawa, and K. Yamada, *Effect of Oil Mist on Tool Temperature in Cutting.* Journal of Manufacturing Science and Engineering, 2006. **128**(1): p. 130.

[4] Yassin, A., et al., *Experimental investigation on cutting mechanism of laser sintered material using small ball end mill.* Journal of Materials Processing Technology, 2009. **209**(15-16): p. 5680-5689.

[5] Jawaid, A., S. Sharif, and S. Koksal, *Evaluation of wear mechanisms of coated carbide tools when face milling titanium alloy.* Journal of Materials Processing Technology, 2000. **99**(1-3): p.266.

Open Science Index, Industrial and Manufacturing Engineering Vol:6, No:11, 2012 publications.waset.org/12176/pdf